# Role of Rubber Dampers in Enhancing NVH Reduction and Thermal Performance in Automotive Engineering

<sup>1</sup>Naiyar Ghayas, <sup>2</sup>Dr Rashmi Dwivedi

<sup>1</sup>Department of Mechanical Engineering, Sri Satya Sai University of Technology and Medical Sciences Sehore (M.P.) India, <sup>2</sup>Department of Mechanical Engineering, Sri Satya Sai University of Technology and Medical Sciences Sehore (M.P.) India,

Email <sup>1</sup>naiyarghayas@gmail.com, <sup>2</sup>rashmidwiyedi29@gmail.com

\* Corresponding Author: Naiyar Ghayas

Abstract: Vehicle comfort and performance are significantly influenced by road driving noise and vibration, necessitating effective mitigation strategies. This study examines the pivotal role of rubber dampers in reducing engine-related Noise, Vibration, and Harshness (NVH) while enhancing thermal performance in modern automotive design. Engine, intake, exhaust, and aerodynamic noises collectively shape the vehicle's acoustic profile and customer satisfaction. Rubber dampers strategically attenuate vibrations from moving components, minimizing noise transmission into the cabin and thereby improving passenger comfort. Furthermore, they contribute to thermal management by mitigating heat transfer, optimizing vehicle efficiency, and enhancing component durability. This research employs numerical simulations and experimental analyses to explore the impact of rubber dampers on NVH and thermal performance, demonstrating their effectiveness in advancing automotive technology.

**Keywords:** Rubber dampers, NVH reduction, thermal management, automotive engineering, engine noise.

#### I. INTRODUCTION

Road driving noise and vibration are significant factors influencing the overall comfort, performance, and perception of vehicles. The automotive industry employs a diverse array of techniques and technologies to analyse and mitigate these issues, ranging from fundamental methodologies to advanced test rigs and instrumentation. Central to this study is the role of rubber dampers in addressing engine-related noise, vibration, and harshness (NVH) while also enhancing thermal performance, a critical consideration in modern vehicle design. The primary sources of noise in road vehicles stem from the engine, manifesting as intake noise, exhaust noise, and mechanical noise. Each contributes uniquely to the overall acoustic profile of the vehicle, influencing its perceived quality and customer satisfaction. In parallel, the resonance of these noises within various vehicle components further amplifies their impact on NVH characteristics. The performance of a vehicle in terms of sound and vibration plays a pivotal role in customer satisfaction, where preferences can vary significantly between aesthetic appeal, reliability, and safety considerations. Sound, particularly, is a paramount factor influencing consumer choice, highlighting the importance of effective NVH management in automotive design.

Air conditioners expanded the space to distribute heat to the surroundings. These extensions are called fins. A larger surface area is needed to remove more heat from these areas. However, in addition to the above requirements, the noise of the blades is also an issue that concerns design engineers. Fins are thin parts used to cool the engine. When the engine runs at high speed, the vanes vibrate and this vibration causes the sound to worsen. So better thermal design of the motor does not mean better design from noise. Based on technology, consumers are now looking for quieter machines for better comfort [2-4]. One method used in the design of air conditioning motors is to place rubber dampers on the fins to reduce the sound of the fins. Although the noise of the jacuzzi can be reduced with this method, the cost will be more. Additionally, the presence of rubber shock absorbers affects the cooling of the engine cylinder head. As the prices of raw materials such as steel and aluminum increase day by day, rubber dampers add additional costs and affect the company's income. Therefore, efforts should be made to create engines that will reduce or eliminate the use of rubber shock absorbers while meeting all the needs of the engine.



Figure 1. Engine cylinder head with rubber dampers (black color) between the fins [5]

#### A. Vehicle noise

Vehicle noise encompasses a broad range of acoustic disturbances originating from various sources within and around the vehicle. Engine noise, a primary contributor, arises from the combustion process and mechanical movements within the engine, including intake and exhaust noise. Aerodynamic noise results from airflow over the vehicle's exterior surfaces, causing turbulent eddies and pressure fluctuations. Additionally, road and tire noise stem from the interaction between tires and road surfaces, generating vibrations and frictional noise. Effective management of these noise sources through engineering solutions such as improved engine design, aerodynamic optimizations, and advancements in tire technology is crucial for enhancing vehicle comfort, performance, and environmental impact.

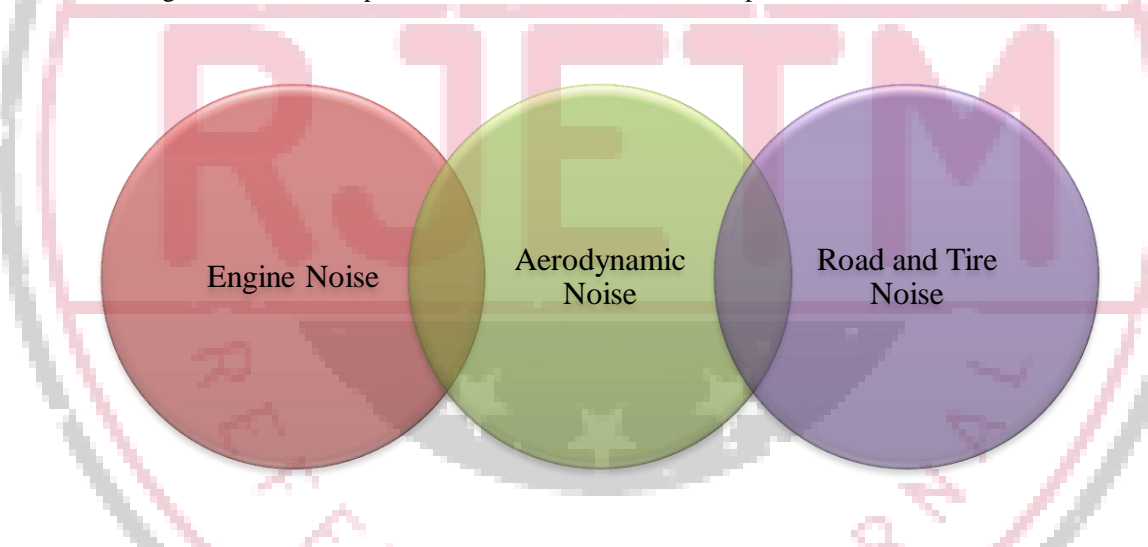


Figure 2 Different types Vehicles Noise

### B. Role of Rubber Dampers in NVH Reduction and Thermal Performance Enhancement

Rubber dampers are integral components in modern automotive design, serving dual purposes of NVH reduction and thermal performance enhancement. Primarily, these dampers are strategically placed throughout vehicles to absorb and dissipate vibrations generated by moving components such as engines, drivetrains, and suspension systems. By isolating these vibrations from the vehicle chassis and body structure, rubber dampers effectively reduce the transmission of noise and vibration into the cabin, thereby enhancing passenger comfort and overall driving experience. This damping capability extends beyond vibrations to encompass noise attenuation, where rubber dampers help mitigate engine noises, gearbox whines, and road-induced vibrations that contribute to interior cabin noise levels.

Furthermore, rubber dampers contribute to thermal management within vehicles by limiting the transfer of heat generated by operational components. By absorbing vibrations that would otherwise conduct heat, they assist in maintaining optimal temperatures for critical systems like engines and transmissions. This thermal regulation not only improves overall vehicle efficiency but also enhances the reliability and durability of key automotive components. Through these combined roles, rubber dampers play a significant part in advancing automotive technology, ensuring quieter, smoother rides while optimizing performance and longevity in modern vehicles.



Figure 3 The Critical Role of Rubber Dampers in New Energy Vehicles

As global demand for new energy vehicles (NEVs) accelerates, their unique design requirements call for innovative solutions from automotive component suppliers. One area where NEVs differ fundamentally from traditional petrol cars is vibration damping. NEVs produce far less noise and vibration from the engine and drivetrain, but are prone to increased cabin noise from wind and road inputs. High-performance shock and vibration damping is crucial to maximize ride comfort and maintain premium vehicle quality.

This is where advanced rubber dampers and isolators play an indispensable role in NEV design. Compared to metal components, rubber dampers provide exceptional noise and vibration isolation across a broad frequency range. With precisely engineered shapes and rubber compounds, our dampers effectively control noise and harshness issues originating from chassis, suspension, and battery systems. Whether absorptive mounts, bushings, or anti-vibration pads, our solutions are proven to isolate NEV cabins and batteries from unwanted vibration.

As a leading damper manufacturer, we are heavily invested in R&D to push the limits of rubber damper technology. We work closely with NEV companies to engineer custom, optimized solutions that enhance the vehicle ownership experience. Going forward, noise control will be a key factor differentiating premium NEVs, and our rubber dampers will play an integral role in enabling superior comfort and refinement. With China projected as the world's largest NEV market, Chinese automakers can rely on our expertise and capabilities to help lead the future of e-mobility.

### C. Sources of variability in automotive systems: material and attachment method uncertainty

One can begin to think about the elements that most influence the system unpredictability once the outer variables have been quantified and it has been established that they have little impact on the internal variety. This may seem overwhelming given the enormous number of parts and procedures required to make a single vehicle, each of which will have corresponding material or manufactured tolerance. As the design is improved in the coming, the geometry complication is anticipated to rise even farther.

It is common knowledge that mounted methods, non-linear polymeric material, and connections like bolts and spot welds are some of the key contributors to variation from vehicle to vehicle. However, because it is impracticable to place a transmitter inside a joint, measurements to assess structural variability at component joints are particularly challenging to conduct. The significant variation in polymeric products is mostly caused by their occasionally non-linear behavior and sensitivity to environmental factors, particularly in materials like rubber. There is a common assumption that the significant (and variable) loss factor is the cause of the high variation in FRFs utilizing viscoelastic materials.

Sealant are crucial for dampening air sound and protecting the passenger's cabin from moisture. As evidenced by engine mounts, the environment and the amount of pre-load applied to polymeric material, such as seals, can drastically alter how they behave. The location of components with polymer seals is of little consequence to the seal behavior, as shown by modeling the forcing applicable to weather strips and other rubber sealers with non-linear solvers; rather, variants in the door's geometrical as well as the updating on the weather strips can cause noticeable differences in the reaction.

The degree of dampening present throughout the device can have an impact on the frequency-dependent fluctuation of polymer material. Material dampening and blankets viscosity dampening will both be used while modeling the door and trim, and the two types will be contrasted. According to earlier research, the wave causes a high level of variation to be present at higher frequency. A glass and polymer-layered windshield was subjected to a low frequencies investigation that tracked environment changes. It was discovered that low frequency variations varied between 3-6%, whilst higher frequencies showed a 19% variability calculated around the mean.

#### II. LITERATURE REVIEW

**Mohamed et al. (2018)** [8]: This study focuses on reducing interior vehicle noise, particularly structure-borne noise from powertrain sources. They utilize transfer path analysis to evaluate noise, vibration, and harshness (NVH) transfer functions, introducing a friction damper on the nearside powertrain mount to mitigate noise levels. Experimental data from a midsize executive car confirms significant reductions in interior noise levels across varying speeds.

**Singh et al. (2014) [9]:** Investigates the application of rubber dampers in internal combustion engines to reduce unwanted noise and vibrations generated by oscillating fins on engine surfaces. The study combines experimental measurements in a semi-anechoic chamber with computational fluid dynamics (CFD) simulations to analyze heat transfer and NVH performance improvements. Results indicate that rubber dampers effectively reduce high-frequency engine noise while maintaining thermal efficiency.

Gao et al. (2024) [10]: Explores the use of tuned rubber mass dampers (TRMD) to enhance dynamic performance in vehicle subframes, crucial for meeting NVH targets. They develop a mathematical model integrating the subframe's finite element analysis (FEA) with TRMD parameters, optimizing the subframe design for robustness against vibrations from rough roads and driver input. The study emphasizes TRMD's cost-effectiveness and efficiency compared to traditional thickness optimization methods.

**Xu et al. (2020)** [11]: Focuses on acrylate viscoelastic dampers designed to dissipate energy under external stress, particularly effective at different temperatures and excitation frequencies. They propose a modified fractional-derivative model to predict the damper's dynamic properties accurately, incorporating temperature and amplitude effects. Experimental results validate the model's efficacy, highlighting the damper's potential for applications requiring precise damping control.

**Sheikhi et al.** (2021) [12]: Analyzes U-shaped dampers integrated with shape memory alloy (SMA) and structural steel (SS) for rubber bearings in high shear strain environments. Using ANSYS modeling, they demonstrate the effectiveness of SMA dampers in reducing residual deformation and enhancing energy dissipation. The study identifies optimal SMA to SS thickness ratios through finite element analysis, providing insights into improving damper performance in structural applications like bridges.

Khiavi et al. (2020) [13]: Discusses the seismic control of concrete dams using rubber shock absorbers, evaluating the impact of shock absorber thickness and height on damping responses. They employ sensitivity analysis and modeling techniques to determine optimal dimensions for maximizing safety and cost-effectiveness in seismic design. Results show that rubber dampers effectively mitigate hydrodynamic pressures and seismic forces, enhancing the durability and performance of concrete dams.

Liu et al. (2023) [14]: propose a hybrid damping strategy combining negative stiffness dampers (NSD) and high damping rubber (HDR) dampers to effectively manage multi-mode vibrations in stay cables. Their study conducts comprehensive modal analyses coupled with asymptotic and iterative solutions to optimize damping configurations, offering versatile solutions for enhancing cable damping across various modal ranges.

Modhej et al. (2023) [16]: investigate viscohyperelastic dampers (VHD) composed of viscoelastic materials and metal strips. Using FEM simulations, they explore how different rubber materials and dimensions impact damper performance. Their findings emphasize the effectiveness of VHD in dissipating energy, highlighting the material's capability to adjust stiffness and damping properties for optimal performance.

Cao & Yi (2021) [17]: introduce a novel damper design utilizing shape memory alloy (SMA) and elastic springs to enhance seismic control in bridges. They validate their approach through analytical methods and simulations, demonstrating the damper's ability to manage small and large displacements effectively. Their design aims to minimize bridge movement during seismic events while ensuring structural integrity and safety.

**Gejguš et al. (2022) [18]:** explore the viscoelastic behavior of elastomeric components in high-frequency applications, such as permanent magnet synchronous motors (PMSM). They compare dynamic stiffness measurement techniques, validating their findings through numerical simulations. Their study provides insights into optimizing elastomer designs for applications requiring precise dynamic stiffness characteristics.

**Hazra & Reddy** (2022) [19]: compare natural rubber (NR) and polyurethane (PU) in electric vehicle powertrain installations to evaluate their NVH characteristics. They highlight PU's superior dynamic stiffness and NVH performance, particularly its effectiveness in controlling engine-induced vibrations and enhancing vehicle comfort. Their study supports PU's growing use in EV powertrains for improved durability and noise reduction.

**Nurchasanah et al. (2023) [20]:** conduct characterization tests on engine mounting rubber (EMR) from different brands to optimize damper designs. They identify an optimal EMR variant based on stiffness and damping ratio tests, aiming to enhance vibration isolation in automotive applications. Their findings contribute to developing more effective EMR solutions that balance performance and cost-effectiveness.

Venczel et al. (2021) [21]: study torsional vibration dampers using visco-dampers in internal combustion engines. They propose design modifications to improve silicone oil durability and heat transfer efficiency, crucial for maintaining damper

performance under varying operating conditions. Their research supports advancements in damping technology for enhancing engine reliability and longevity.

### IV. OBJECTIVES

The objectives of this thesis therefore include:

- 1. The understanding of current NVH optimisation methods to determine areas in which development is necessary.
- 2. To investigate the effect of rubber dampers to eliminate the NVH from the engines with better thermal performances.
- 3. To study modal analysis on various designs for NVH characteristics improvement.

#### IV METHODOLOGY

### A. Frequency Response Function (FRF)

The system that is emitting the signal can be described using acoustic signals. A frequency-response function is the most often used representation of the system (FRF). This is the ratio of the force-based input signal to the velocity-based outputs result. An FRF can employ displacement, velocity, or acceleration units for each force unit. The following equations, which are referred to as the receptance, mobility, and accelerance for the equations, respectively, can be used to characterize the FRF output.  $\bf R$  is the receptance, which may be calculated using displacement  $\bf S$  and the forcing input  $\bf F_{in}$  whilst in the frequency domain. This is denoted by  $\bf \alpha$ , which is the angular frequency. The mobility,  $\bf M$ , is calculated using the velocity output,  $\bf V_{out}$  and forcing input,  $\bf F_{in}$ . The accelerance  $\bf A_{acc}$  is calculated using the acceleration output as well as the forcing input. Finally,  $\bf t$  is the time and  $\bf i$  denotes the complex number.

$$R(\alpha) = \frac{S(\alpha)e^{i\alpha t}}{F_{in}(\alpha)e^{i\alpha t}}$$
(4.1)

$$M(\alpha) = \frac{V_{\text{out}}(\alpha)e^{i\alpha t}}{F_{\text{in}}(\alpha)e^{i\alpha t}}$$
(4.2)

$$A_{acc}(\alpha) = \frac{A_{acc}(\alpha)e^{i\alpha t}}{F_{in}(\alpha)e^{i\alpha t}}$$
(4.3)

Every component within a system possesses a natural frequency determined by its geometry and boundary conditions. When an external force's frequency aligns with a component's natural frequency, resonance occurs, resulting in heightened displacement compared to other frequencies. Resonances manifest as peaks in mobility plots, known as modes, with corresponding periodic deformations termed mode shapes, typically extracted through eigenvectors.

To mitigate resonant peaks, damping can be applied, and design alterations can shift natural frequencies away from critical frequency bands. Changes in shape or system properties influence mode positioning and amplitude, while coupling between components can also alter resonant frequencies. Statistical approaches, such as applying a spread to Frequency Response Functions (FRFs), quantify system variability. Similar methods apply to acoustic responses, often focusing on sound power levels instead of FRFs.

Along transmission paths, noise transfer can be managed via damping techniques, redirection, or destructive interference, where resonance peaks are aligned with anti-resonances. Finite Element Simulation (FEA) is a primary method for high-fidelity modeling, accommodating complex structures and generating transfer functions for various input-output configurations. Statistical Energy Analysis (SEA) offers computational efficiency but requires deeper physical insight from operators compared to FEA.

#### **B.** Finite Element Analysis

Finite element analysis is a tool used to solve various engineering problems in industrial applications is quite a new concept. It is also use for calculations, models and simulations to predict and understand how an object might behave under various physical conditions.

### **ANSYS Capabilities:**

In FEM (finite element analysis) ANSYS software is used that helps engineers for performing the following works:

• To build computer prototype, components, transfer CAD model structures in a system products.

- Enhances the profile of structural member with shape optimization.
- To study stress levels, temperature distributions.
- To reduce production costs design should be optimized in early development process.
- Prototypes are tested under normal conditions when it would not be practical or desirable to do so (biomedical applications, for example).

The ANSYS graphical user interface (GUI) provides users with a simple, interactive way to access software functionalities, documentation, commands, and reference materials. Users interact with the ANSYS program using an easy-to-use menu system. Data can be entered using a mouse, a keyboard, or both in tandem.

### C. Analysis Steps in ANSYS

The different analysis steps involved in ANSYS are mentioned below.

#### I. Preprocessor

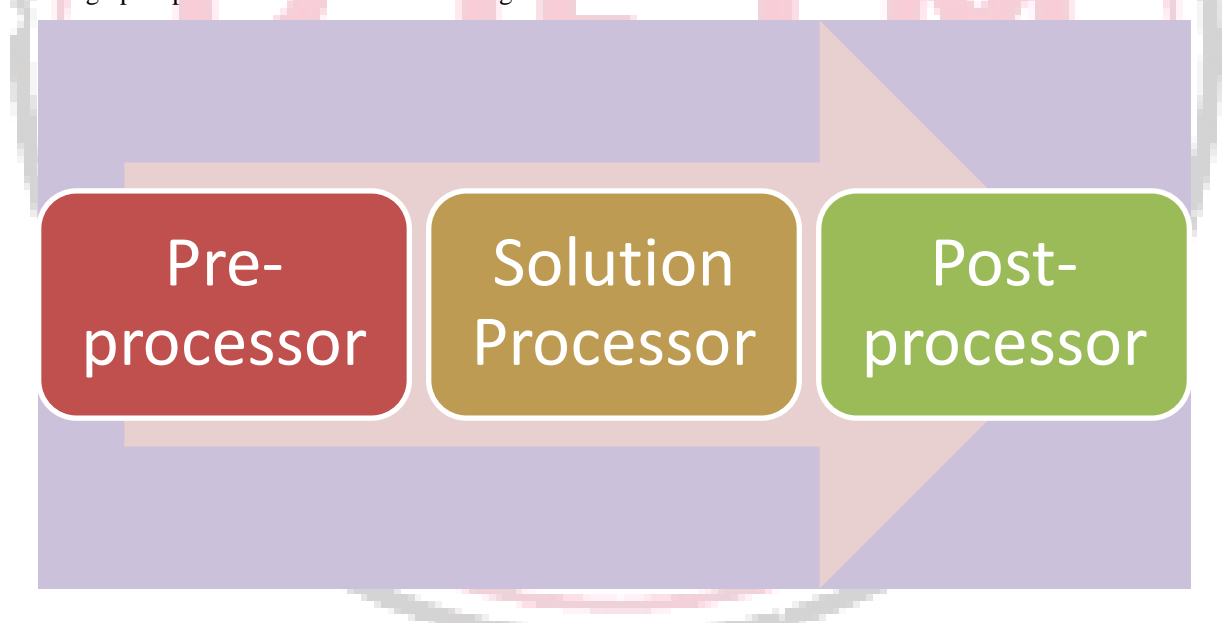
The model setup is basically done in preprocessor. The different steps in pre-processing are

- Build the model
- Define materials
- Generation of element mesh

#### **II. Solution Processor**

Here, the issue is remedied by compiling all the necessary information about the issue. In this stage of the study, the finite element approach instantly generates an equation, which the computer takes over and solves. Nodal degree of freedom values, which define the first solution derived values that form the component, are the solution's results.

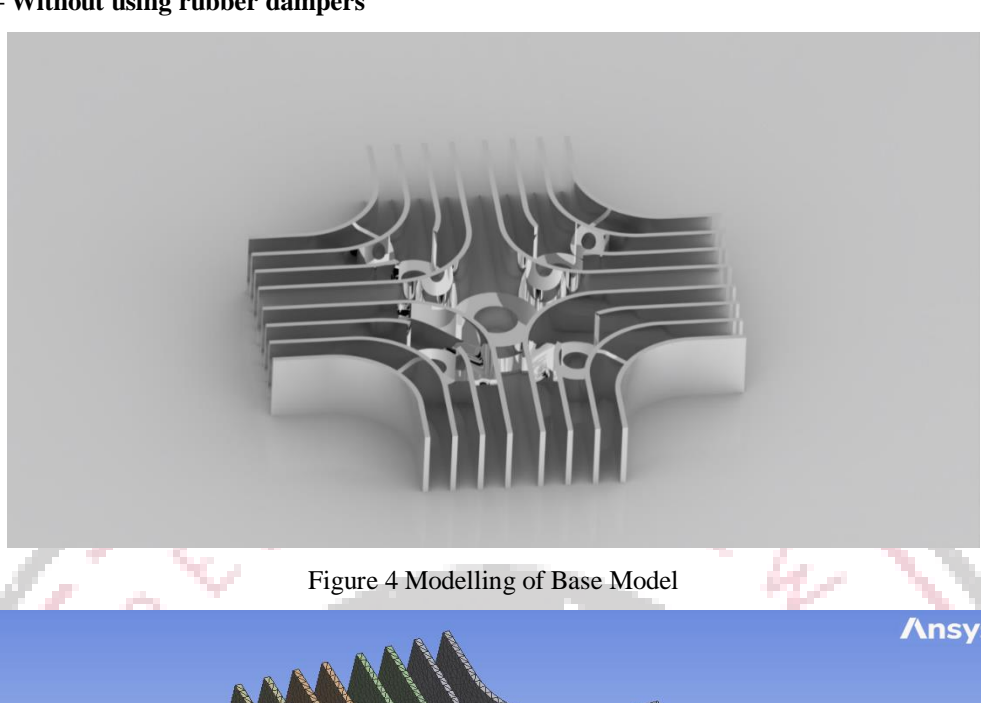
III. Postprocessor: The generic postprocessor completes the task of reviewing analytical results across the entire model. A postprocessor can perform a wide range of complex information manipulation tasks, such as combining load cases, in addition to graphic presentations and tabular listings.



## D. Modelling and Meshing of the models

Modal analysis in structural mechanics is employed to ascertain the natural mode shapes and frequencies of a structure under free vibration conditions. It provides crucial insights into the fundamental causes of vibration issues. Typically, the lowest frequencies are of particular interest because they often represent the predominant modes of vibration, overshadowing higher frequency modes. These modes are intrinsic characteristics of a structure and are dictated by its material properties (mass, damping, stiffness) and boundary conditions. Changes in material properties, structural design, or boundary conditions can alter these modes. During modal analysis, damping effects and external forces are typically disregarded to focus solely on the inherent characteristics of the structure. In this study, a finite element model of the cylinder head was developed using ANSYS software, excluding rubber dampers from the initial simulations. The inclusion of rubber would necessitate nonlinear analysis, which demands significant computational resources and time.

# Base Model – Without using rubber dampers



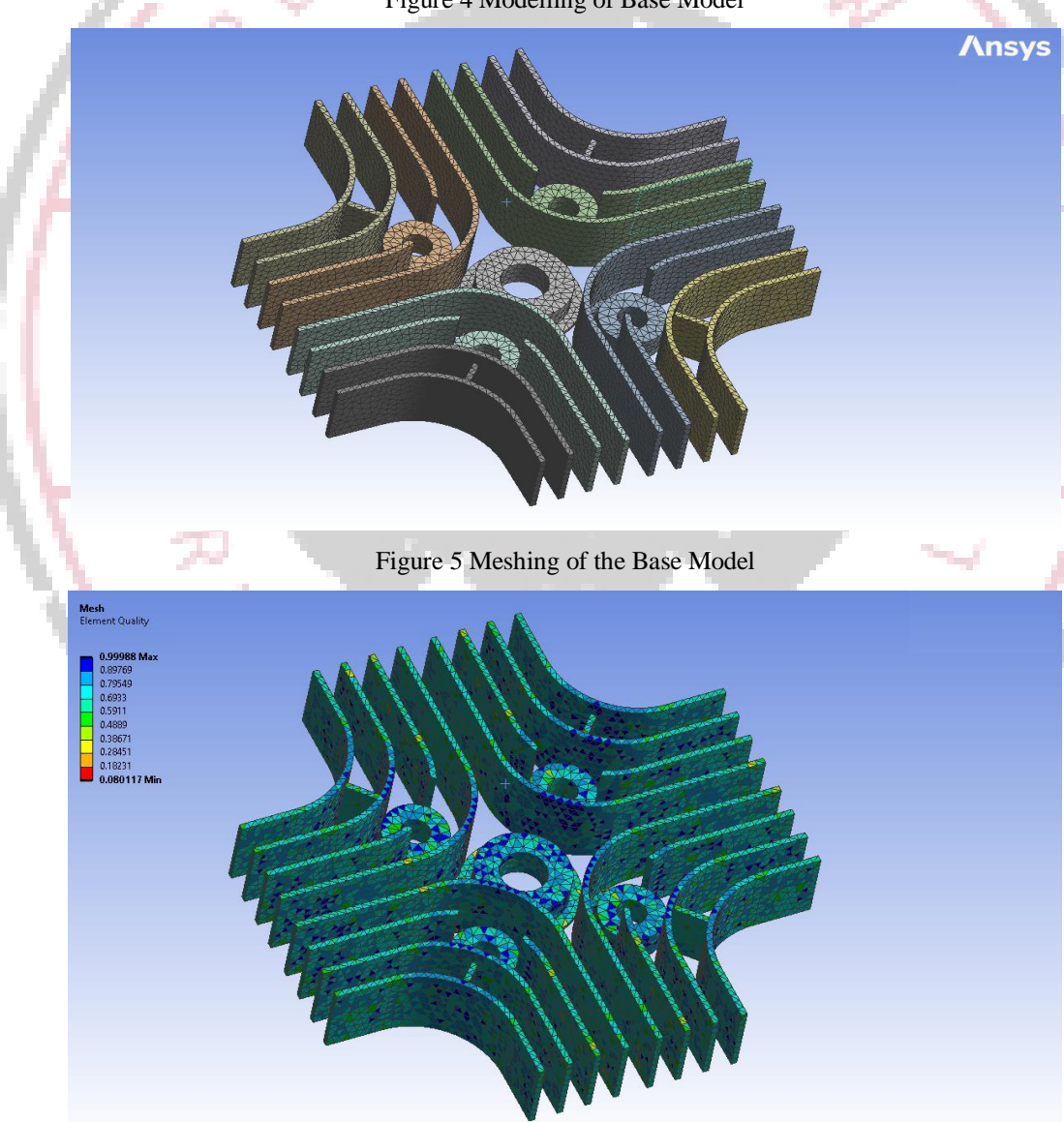


Figure 6 Mesh Element Quality of Base Model

In base model which is without damper, the minimum number of elements used in mesh are 0.080117 and maximum number of elements used are given as 0.99988.

# Case 1 – Placing the rubber dampers inside the engine head

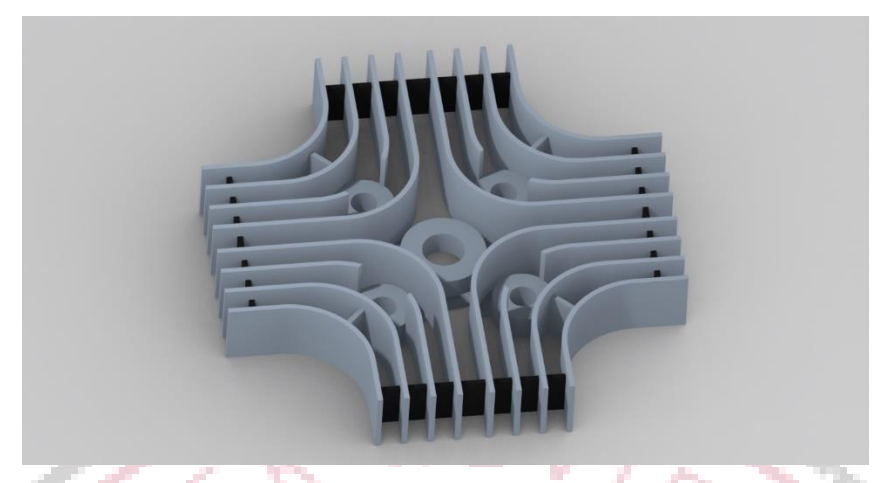


Figure 7 Modelling of modified model case 1 having rubber dampers

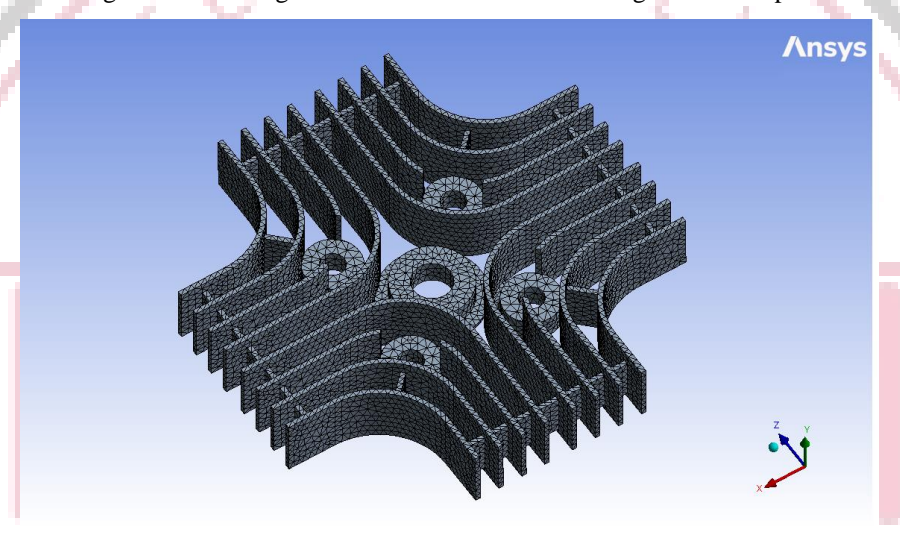


Figure 8 Meshing of modified model case 1 having rubber dampers

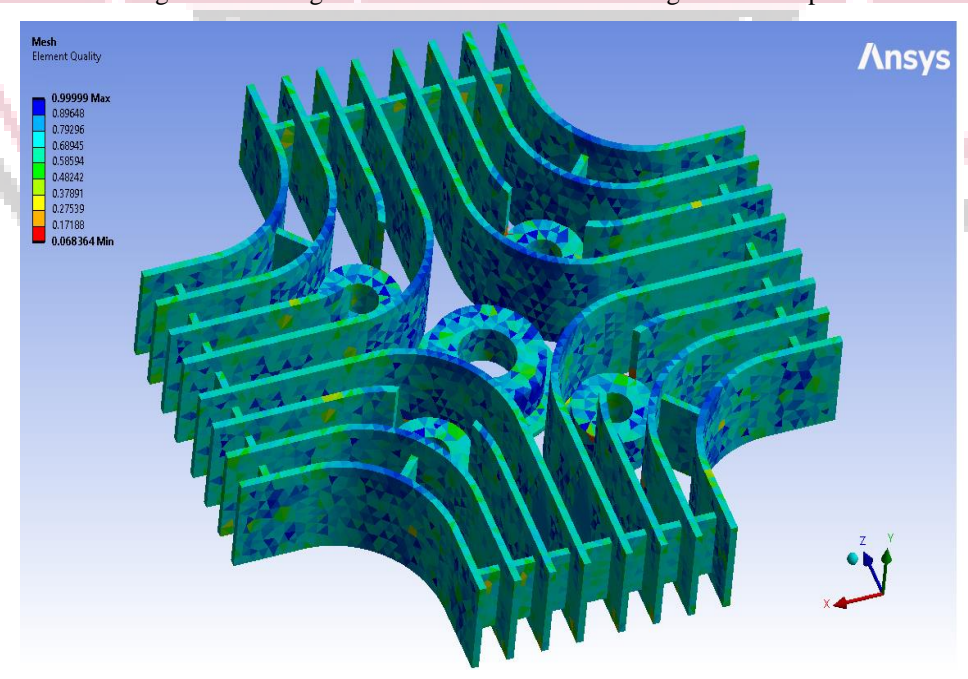


Figure 9 Mesh Element Quality of modified model case 1 having rubber dampers

In proposed model case 1 which is having rubber damper, the minimum number of elements used in mesh are 0.068364 and maximum number of elements used are given as 0.99999.

# Case 2 – Modification in Configurationof rubber dampers in engine head

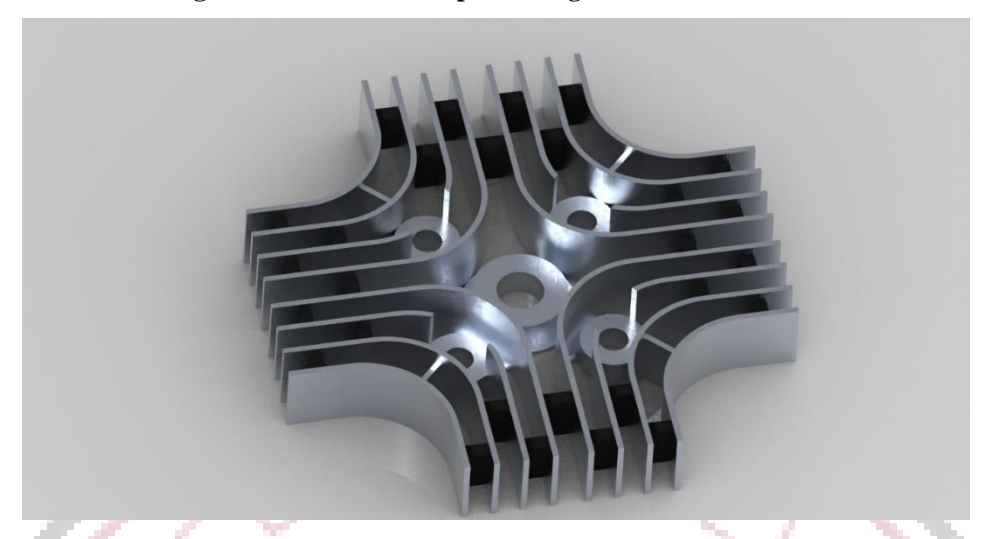


Figure 10 Modelling of modified model case 2 having rubber dampers

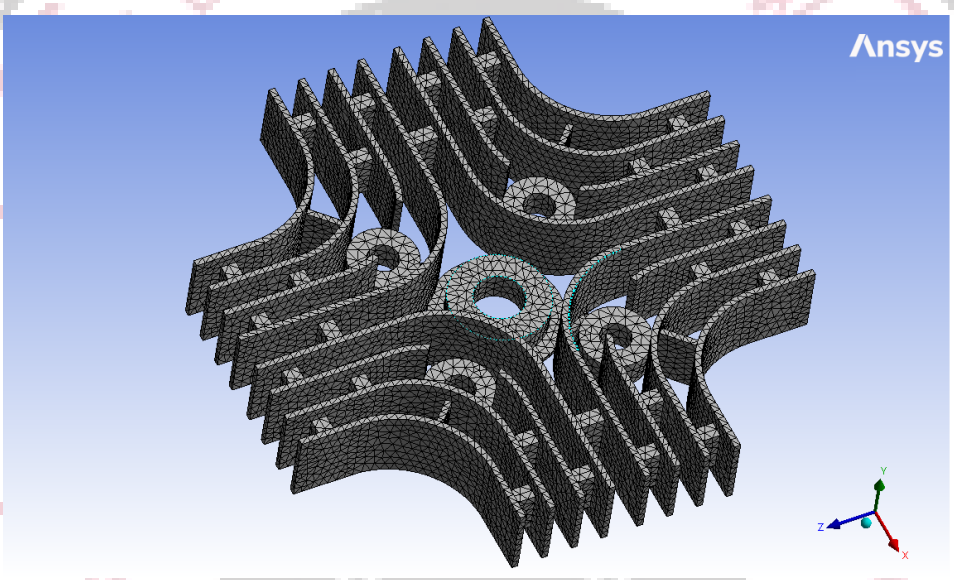


Figure 11 Meshing of modified model case 2 having rubber dampers

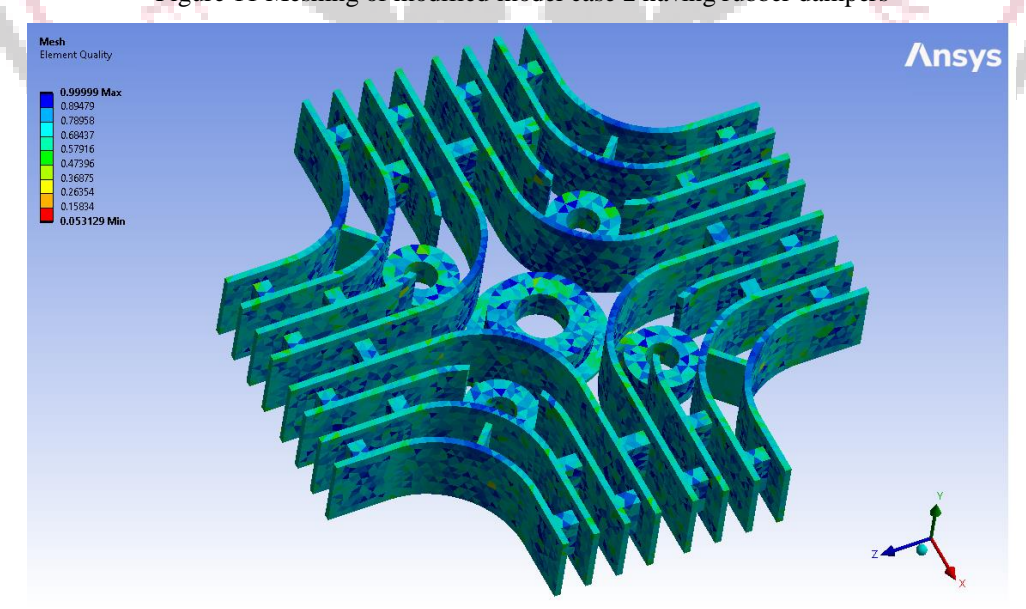


Figure 12 Mesh Element Quality of modified model case 2 having rubber dampers

In proposed model case 2 which is having rubber damper at modified position, the minimum number of elements used in mesh are 0.053129 and maximum number of elements used are given as 0.99999.

# 4.5.4 Case 3 – Modification in Configurationof rubber dampers in engine head

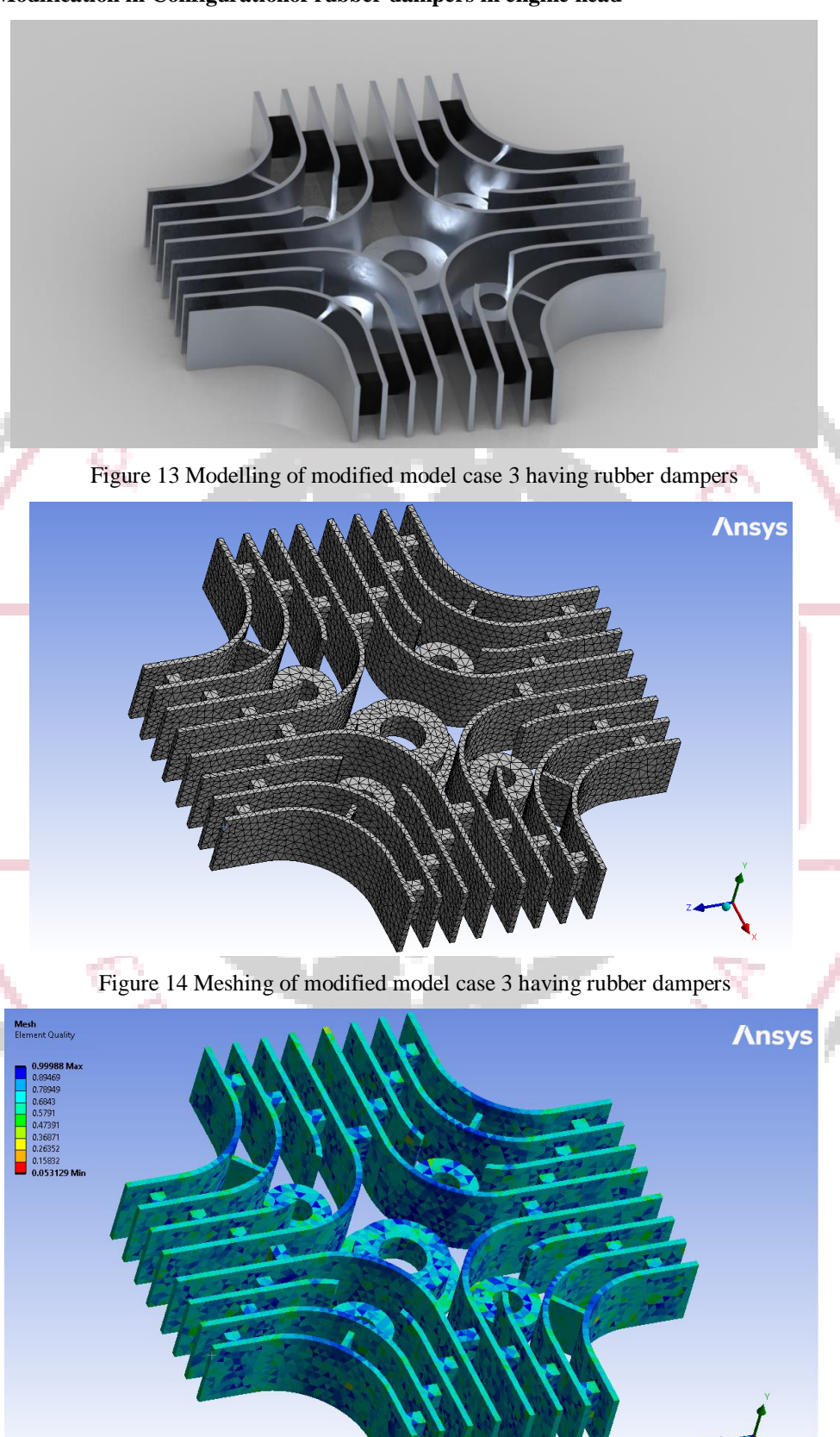


Figure 15 Mesh Element Quality of modified model case 3 having rubber dampers

In proposed model case 3 which is having rubber damper at modified position, the minimum number of elements used in mesh are 0.053129 and maximum number of elements used are given as 0.99988 in above figure 4.12

# Case 4 - Modification in Configuration of rubber dampers in engine head

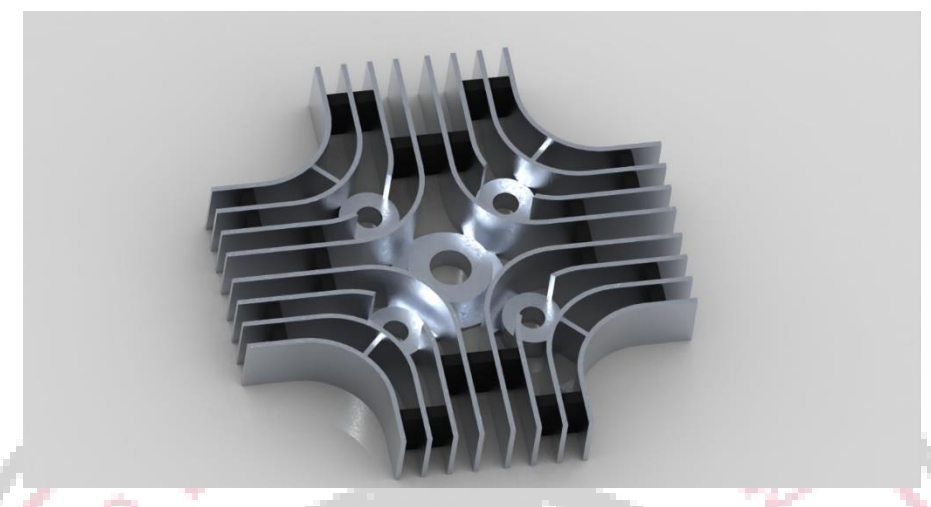


Figure 16 Modelling of modified model case 4 having rubber dampers

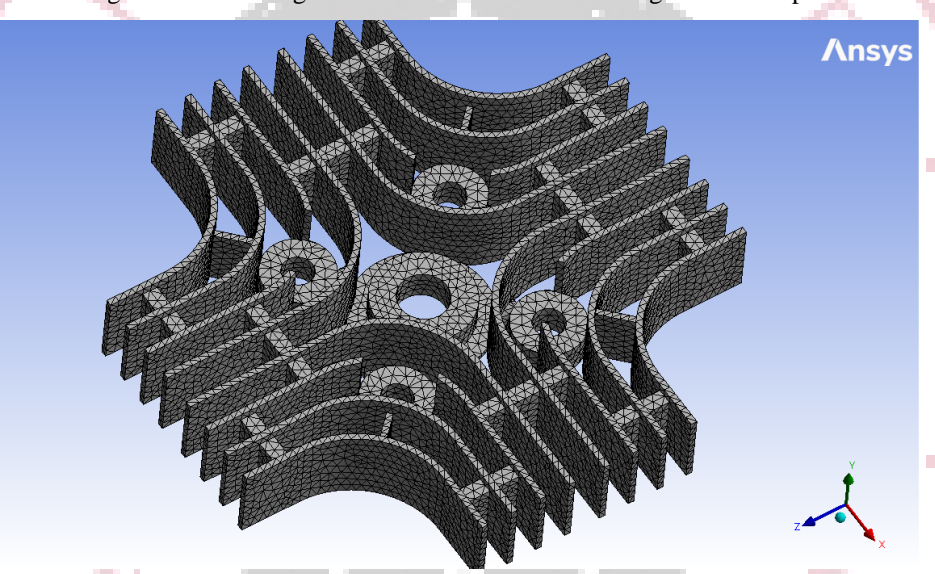


Figure 17 Meshing of modified model case 4 having rubber dampers

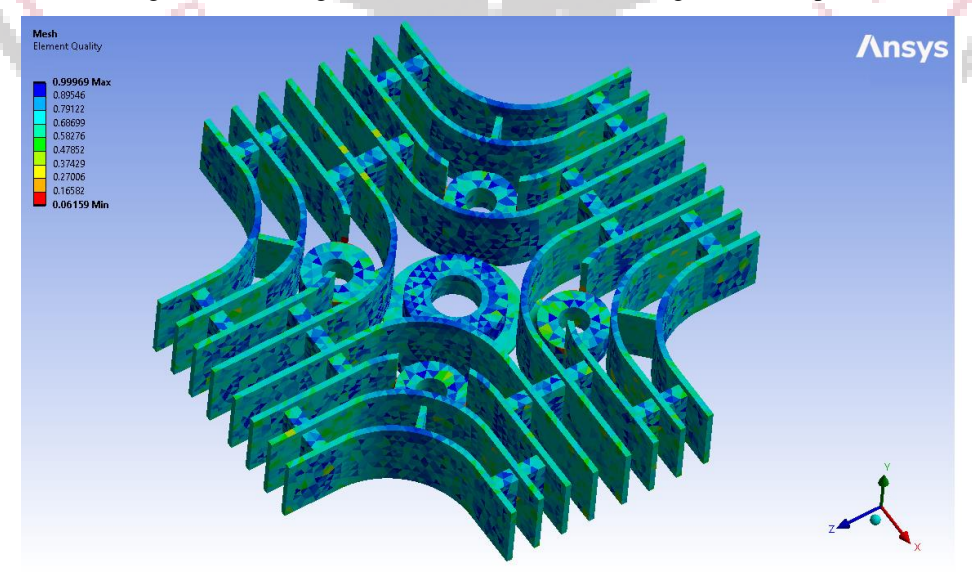


Figure 18 Mesh Element Quality of modified model case 4 having rubber dampers

In proposed model case 3 which is having rubber damper at modified position, the minimum number of elements used in mesh are 0.06159 and maximum number of elements used are given as 0.99969 in above figure 4.15

### 4.6 Material Properties of Aluminium

Table 1 Material Properties of Aluminium

Properties	Aluminium
Tensile strength (MPa)	125
Poisson's Ratio	0.3
Elastic Modulus	70300
Density (Kg/m <sup>3</sup> )	2970

### 4.7 Boundary Condition

- The vehicle velocity was set to 40 km/hr at the inlet, while the static pressure (ambient value) was specified at the outlet of the wind tunnel.
- A constant heat flux boundary condition was applied to the engine liner and combustion chamber, equivalent to 50% of the maximum engine Brake Horsepower (BHP) as thermal load.
- This heat flux was divided into two parts: 70% was applied to the combustion chamber, distributed by the surface area of the chamber, and the remaining 30% was applied to 70% of the liner's surface area.
- The bottom 30% of the liner was designated as an adiabatic boundary wall.
- Contact resistance between the fins and dampers was not considered.
- To validate these boundary conditions, a full vehicle Computational Fluid Dynamics (CFD) model was constructed, although the primary focus of this study was to investigate the impact of rubber dampers.

# 4.8 Mesh independent test

Achieving mesh independence is crucial for ensuring the accuracy of numerical simulations, as the grid density directly affects truncation errors and the overall validity of results. However, using an excessively dense mesh can lead to unnecessary computational resource usage. In practical applications, a common approach is to incrementally increase the grid resolution by a defined ratio and compare the results between successive meshes. Once the differences in results between these meshes become negligible, the mesh can be deemed sufficiently independent. This strategy optimizes computational resources effectively while ensuring that the results remain reasonable and reliable.

Table 2 Mesh Independent Test Report

Mesh Independent Test Report	
No. of Elements	Frequency (Hz) mode No. 5
1245	19.24.50
6294	1929.80
11202	1933.40
41797	1936.70
55764	1936.71

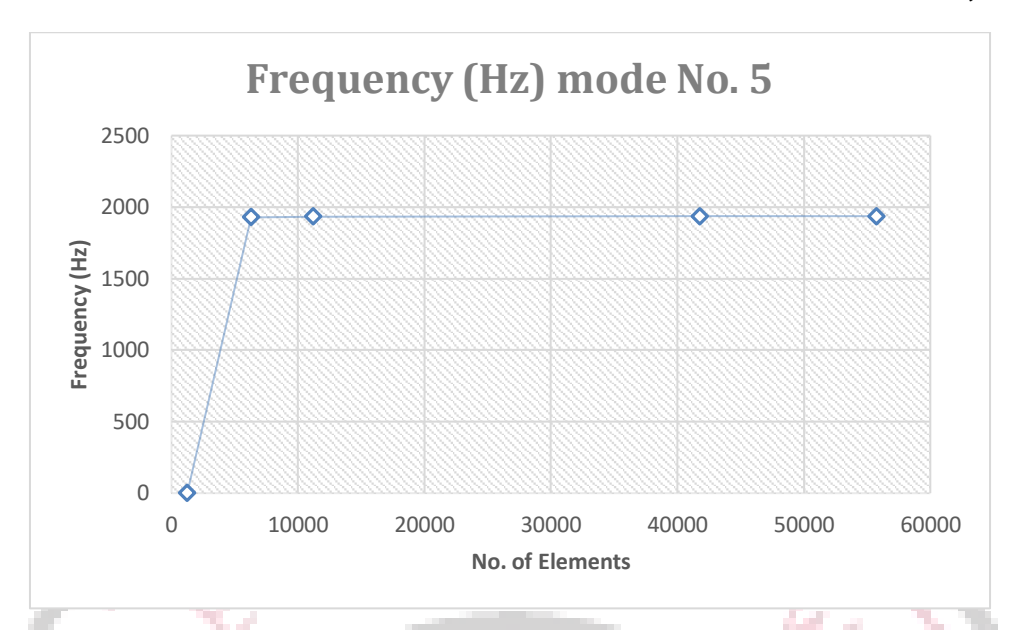


Figure 19 Graphical Analysis of Mesh Independent Test

The above graph shows that the number of elements and frequency is directly proportional to each other. This means that, as the number of elements increases the value of frequency also increases

#### V. RESULT AND DISCUSSION

Previous chapter shows the various design modifications investigated in this research work and now in this chapter we will show the figures corresponding 5<sup>th</sup>mode of vibrations of the cylinder head obtained from the modalanalysis. The subsequent design modifications were based on theresults of the previous designs. Values of the first & fifth natural frequencies and their percentage increase from the base design. First 15 natural frequencies are extracted for each design (see Tables given below).

### A. Modal Analysis for Frequency in Base model

As clearly seen in table 5.1 and graph 5.1, at mode 1, the value of frequency is 1563.7 (Hz) and as the number of iterations increases value of frequency also increases at 7<sup>th</sup> mode the value increases upto 2079.1 (Hz) and in 15<sup>th</sup> mode it reaches upto 3305.0(Hz).

Table 3 Frequency (Hz) at different mode no. for configuration of Base Model

MODE NO	BASE MODEL
1	1563.7
2	1589.6
3	1624.4
4	1626.3
5	1936.7
6	1979.3
7	2079.1
8	2085.0
9	2216.0
10	2218.6

11	2336.2
12	2590.1
13	3180.5
14	3302.8
15	3305.0

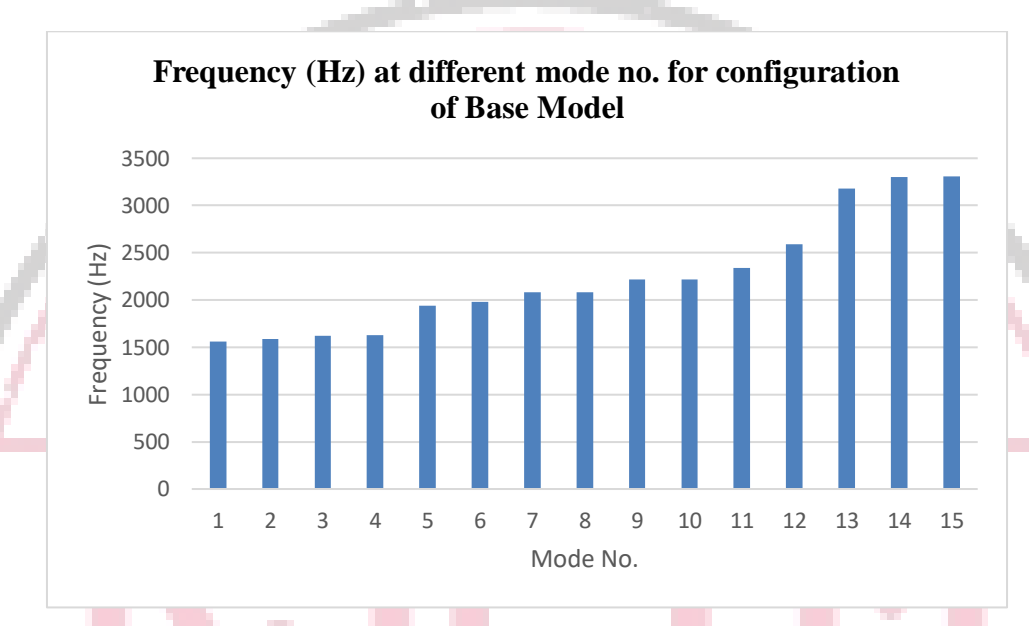


Figure 20 Graphical representation of frequency at different mode no. for base model

# B. Modal Analysis for Frequency in Model Designed in Case 1

As clearly seen in table 5.2 and graph 5.2, at mode 1, the value of frequency is 4134.0 (Hz) and as the number of iterations increases value of frequency also increases at 7<sup>th</sup> mode the value increases upto 5726.1 (Hz) and in 15<sup>th</sup> mode it reaches upto 9796.5(Hz).

Table 4 Frequency (Hz) at different mode no. for configuration of Model in case 1

MODE NO	CASE 1
1	4134.0
2	4203.6
3	4297.7
4	4302.7
5	5317.8
6	5437.3
7	5726.1
8	5742.2

9	6127.4
10	6134.5
11	6477.8
12	7267.6
13	9413.7
14	9790.1
15	9796.5

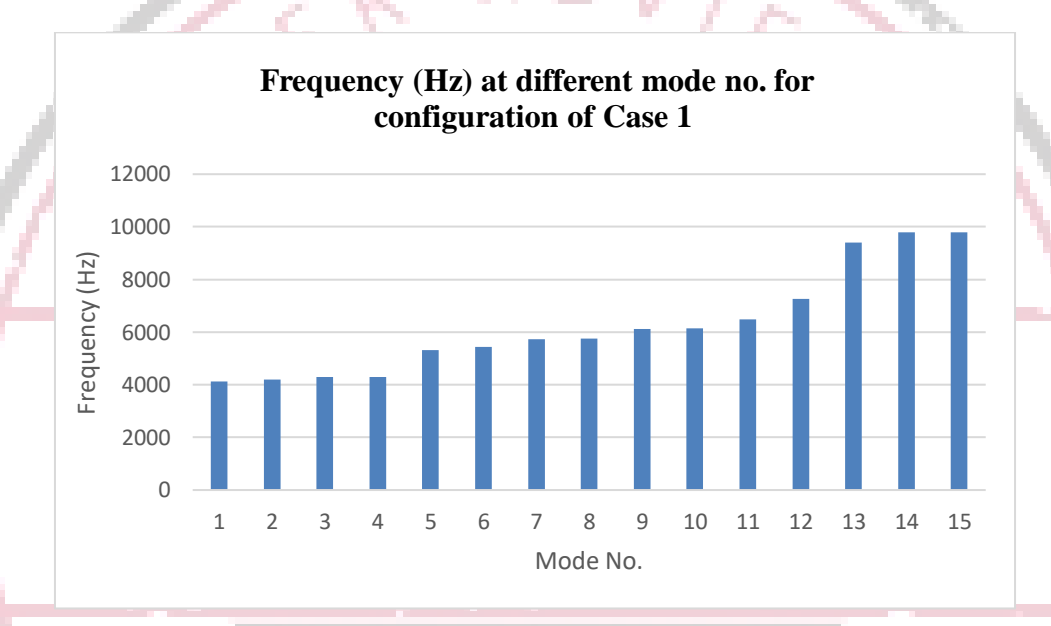


Figure 21 Graphical representation of frequency at different mode no. for Case 1

# C. Modal Analysis for Frequency in Model Designed in Case 2

As clearly seen in table 5.3 and graph 5.3, at mode 2, the value of frequency is 3481.5 (Hz) and as the number of iterations increases value of frequency also increases at 7<sup>th</sup> mode the value increases upto 4629.0 (Hz) and in 15<sup>th</sup> mode it reaches upto 7358.2 (Hz).

Table 5 Frequency (Hz) at different mode no. for configuration of Model in case 2

MODE NO	CASE 2
1	3481.5
2	3539.1
3	3616.6
4	3620.8
5	4312.0
6	4406.7
7	4629.0

8	4642.0
9	4933.8
10	4939.5
11	5201.3
12	5766.5
13	7081.1
14	7353.4
15	7358.2

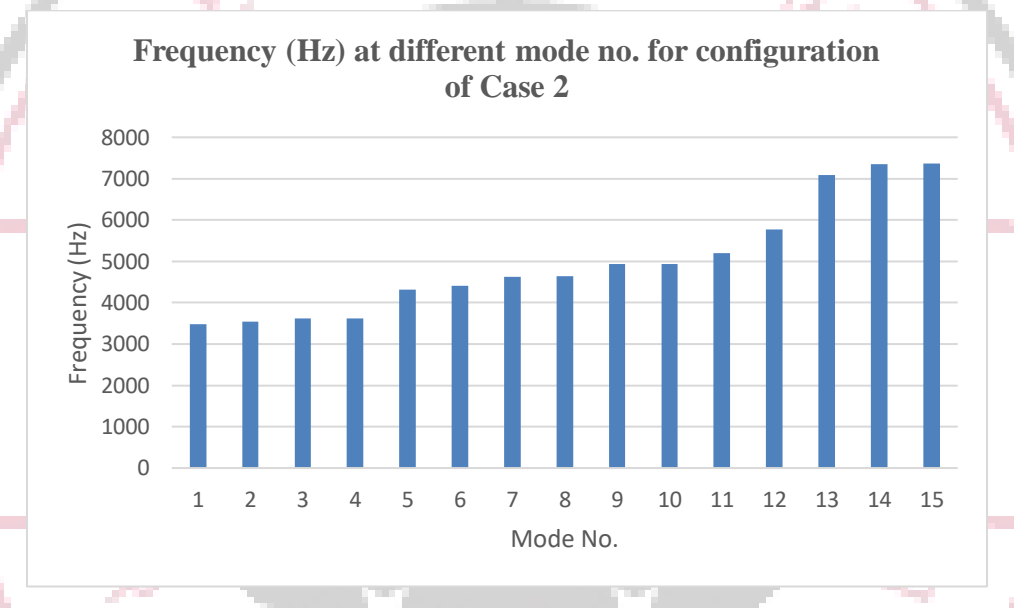


Figure 22 Graphical representation of frequency at different mode no. for Case 2

### D. Modal Analysis for Frequency in Model Designed in Case 3

As clearly seen in table 5.3 and graph 5.3, at mode 1, the value of frequency is 5084.7 (Hz) and as the number of iterations increases value of frequency also increases at 7<sup>th</sup> mode the value increases upto 6760.7 (Hz) and in 15<sup>th</sup> mode it reaches upto 10746.7(Hz).

Table 6 Frequency (Hz) at different mode no. for configuration of Model in case 3

MODE NO	CASE 3
1	5084.7
2	5168.9
3	5282.1
4	5288.2
5	6297.7
6	6436.1

7	6760.7
8	6779.7
9	7205.9
10	7214.2
11	7596.5
12	8422.1
13	10342.1
14	10739.7
15	10746.7

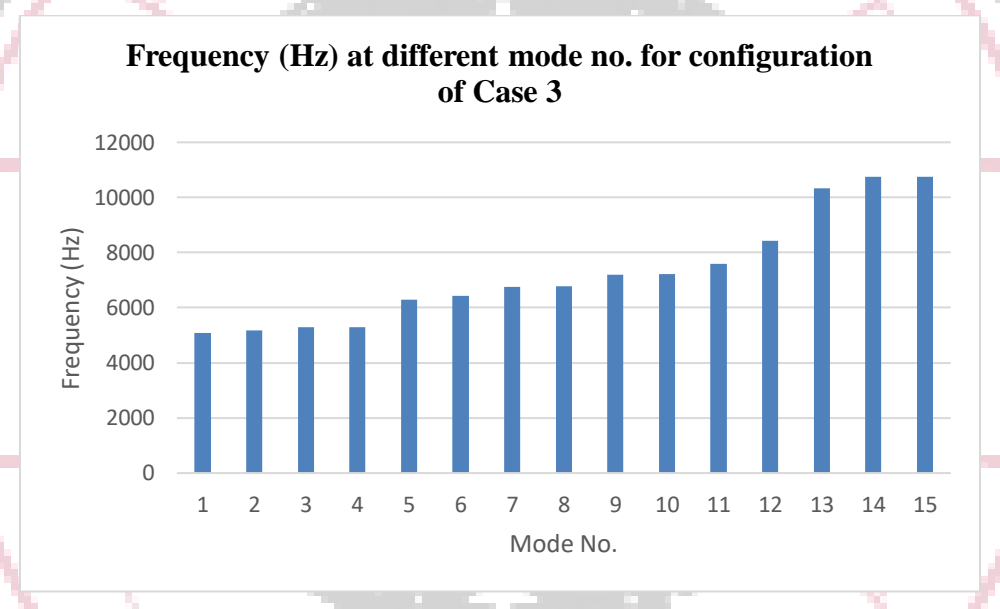


Figure 23 Graphical representation of frequency at different mode no. for Case 3

# E. Modal Analysis for Frequency in Model Designed in Case 4

As clearly seen in table 5.5 and graph 5.5, at mode 1, the value of frequency is 6546.2 (Hz) and as the number of iterations increases value of frequency also increases at 7<sup>th</sup> mode the value increases upto 8703.9 (Hz) and in 15<sup>th</sup> mode it reaches upto 13835.7 (Hz).

Table 7 Frequency (Hz) at different mode no. for configuration of Model in case 4

MODE NO	CASE 4
1	6546.2
2	6654.6
3	6800.3
4	6808.2
5	8107.8

6	8286.0
7	8703.9
8	8728.3
9	9277.0
10	9287.8
11	9780.0
12	10842.8
13	13314.7
14	13826.7
15	13835.7

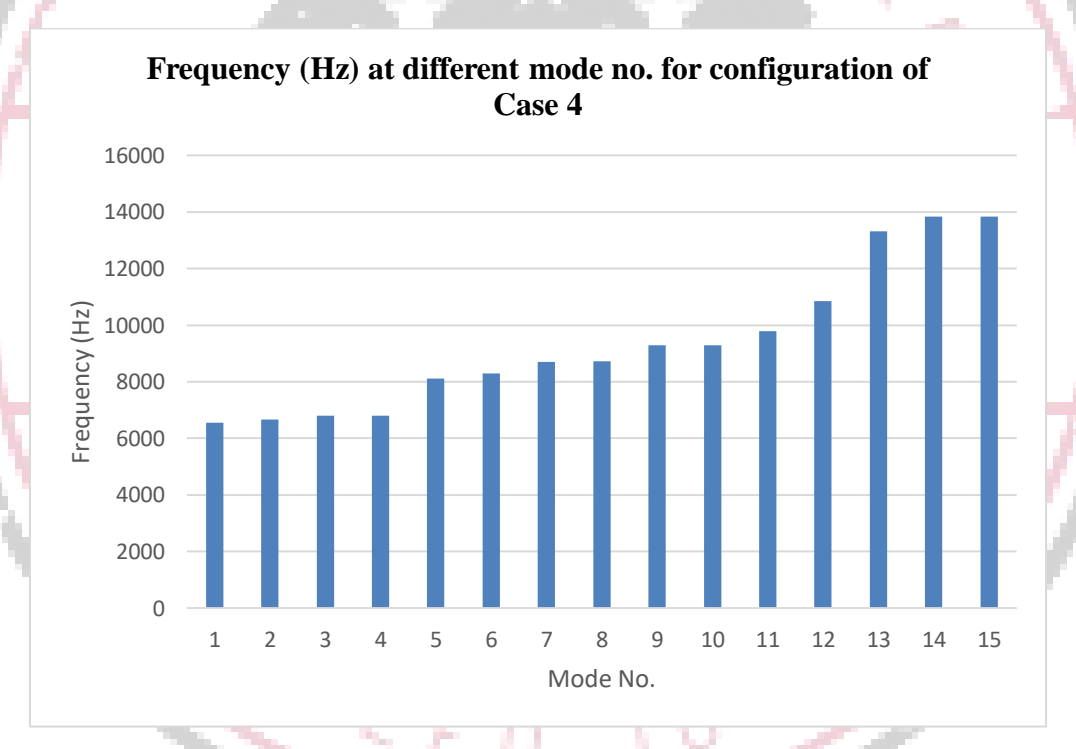


Figure 24 Graphical representation of frequency at different mode no. for Case 4

# F. Comparative analysis of all the cases

Table 8 Frequency (Hz) at different mode no. for configuration of Model in all the cases

Frequency (Hz) at mode no. for different configuration							
MODE NO	BASE MODEL	CASE 1	CASE 2	CASE 3	CASE 4		
1	1563.7	4134.0	3481.5	5084.7	6546.2		
2	1589.6	4203.6	3539.1	5168.9	6654.6		
3	1624.4	4297.7	3616.6	5282.1	6800.3		

4	1626.3	4302.7	3620.8	5288.2	6808.2
5	1936.7	5317.8	4312.0	6297.7	8107.8
6	1979.3	5437.3	4406.7	6436.1	8286.0
7	2079.1	5726.1	4629.0	6760.7	8703.9
8	2085.0	5742.2	4642.0	6779.7	8728.3
9	2216.0	6127.4	4933.8	7205.9	9277.0
10	2218.6	6134.5	4939.5	7214.2	9287.8
11	2336.2	6477.8	5201.3	7596.5	9780.0
12	2590.1	7267.6	5766.5	8422.1	10842.8
13	3180.5	9413.7	7081.1	10342.1	13314.7
14	3302.8	9790.1	7353.4	10739.7	13826.7
15	3305.0	9796.5	7358.2	10746.7	13835.7

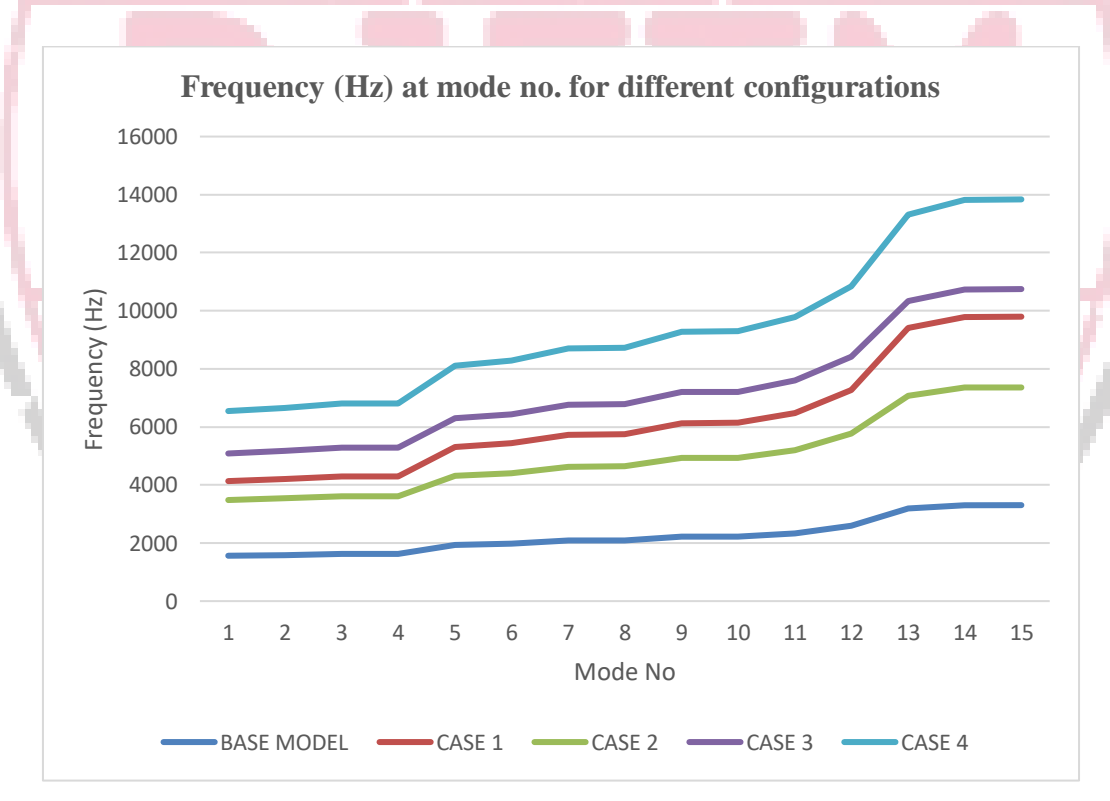


Figure 25 Graphical representation of frequency at different mode no. for all the cases

The initial natural frequency of Design 1 was 1563.7 Hz, which was deemed too low. Consequently, subsequent designs aimed to raise the first mode frequency above 4000 Hz, as frequencies above this threshold are less perceptible to the human ear. At this frequency, it was observed that the centrally located fins exhibited local bending modes of vibration, potentially leading to increased noise levels at resonance. Remarkably, all 15 vibration modes in Design 1 displayed local modes. In Design 2, the introduction of rubber dampers resulted in a significant increase in the first natural frequency to 4134.0 Hz, representing a 100% improvement over Design 1. Fins in this configuration exhibited twisting modes centered around the cylinder head. In Design 3, adjustments were made to the rubber damper placement to mitigate local twisting modes of vibration, resulting in a reduction of the first natural frequency to 3481.5 Hz. Subsequent refinements in Designs

4 and 5 further altered the damper positions, resulting in first mode natural frequencies of 5084.7 Hz and 6546.2 Hz respectively, surpassing those of Designs 1, 2, and 3.

### 5.8 Fifth Mode Deformation for all the models

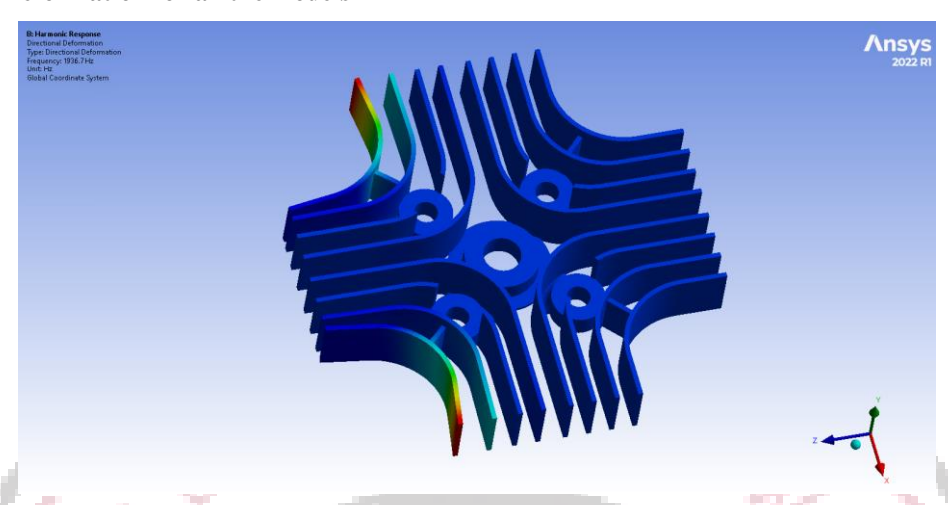


Figure 26 Fifth mode deformation for base model

The above figure shows the fifth mode deformation for base model, which depicts that deformation takes place at 1936.7 (Hz).

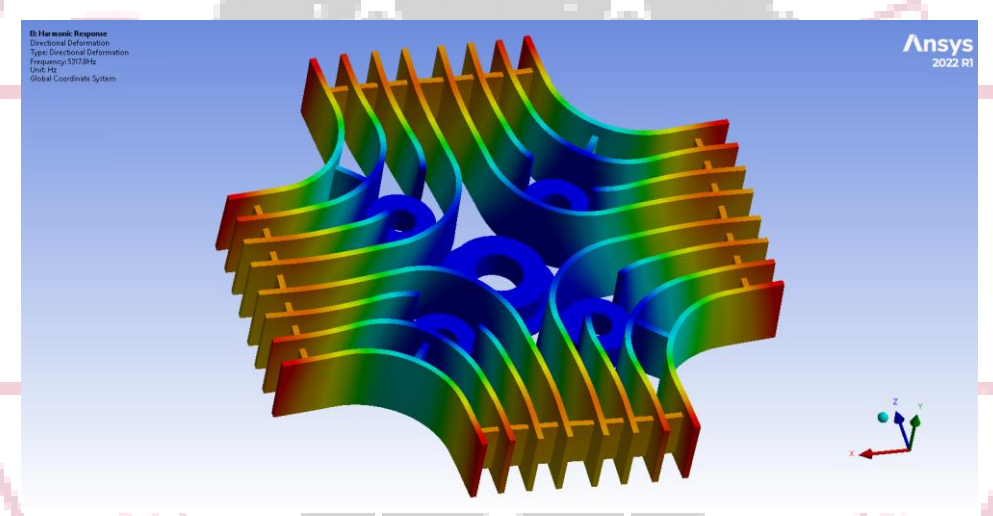


Figure 27 Fifth mode deformation for case 1

The above figure shows the fifth mode deformation formodel in case 1, which depicts that deformation takes place at 5317.8 (Hz).

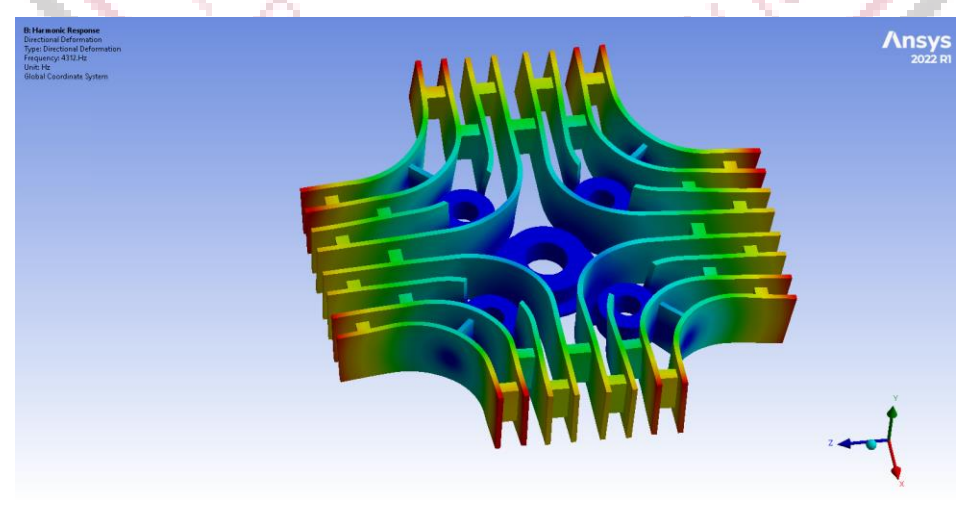


Figure 28 Fifth mode deformation for case 2

The above figure shows the fifth mode deformation formodel in case 2, which depicts that deformation takes place at 4312 (Hz).

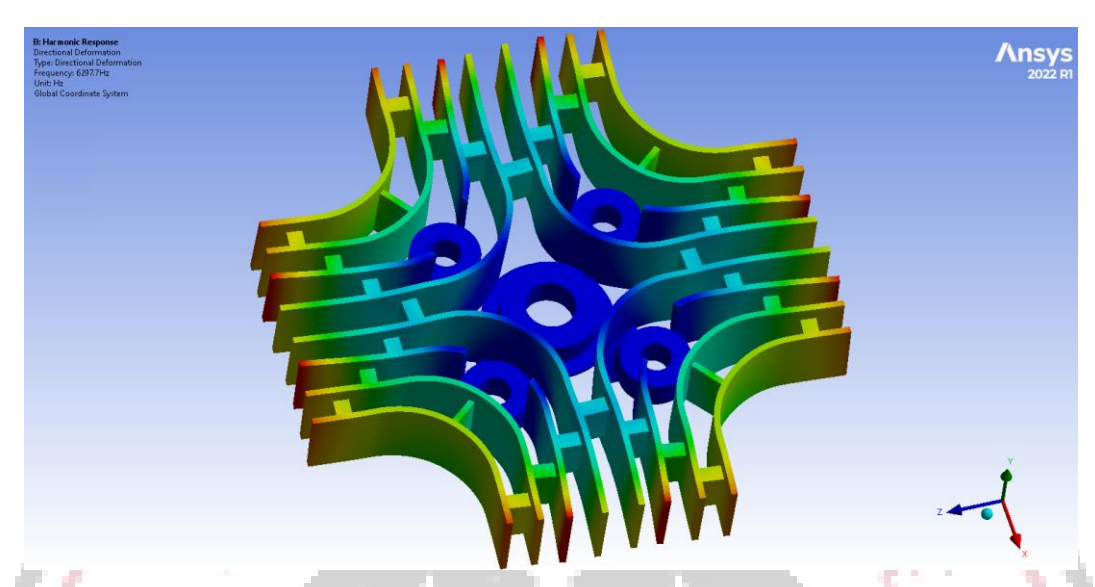


Figure 29 Fifth mode deformation for case 3

The above figure shows the fifth mode deformation formodel in case 3, which depicts that deformation takes place at 6297.7 (Hz).

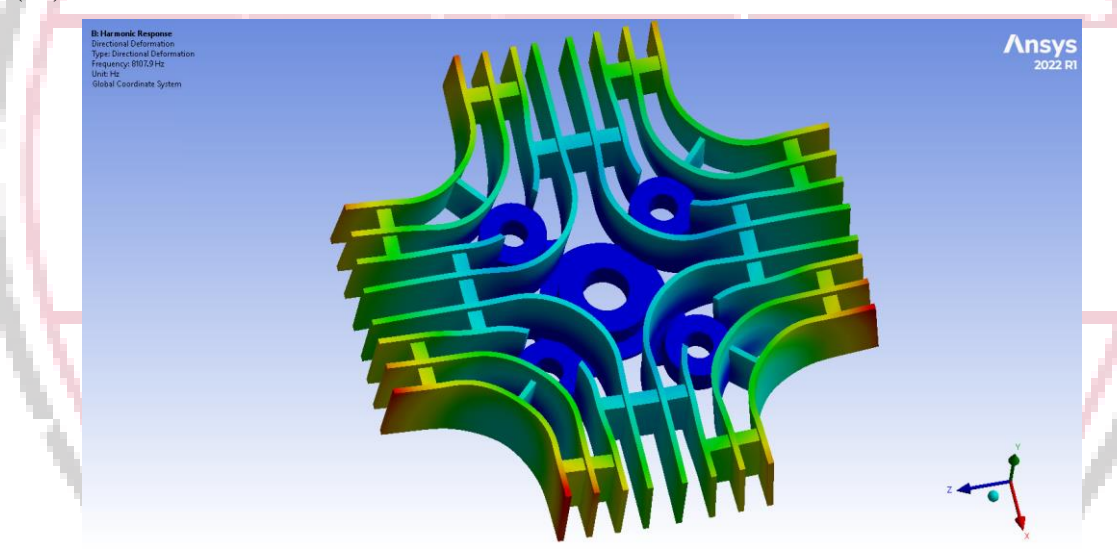


Figure 30 Fifth mode deformation for case 4

The above figure shows the fifth mode deformation formodel in case 4, which depicts that deformation takes place at 8107.9(Hz).

# 5.9 Comparative assessment of deformation in all the models at mode 5

Table 9 Frequency (Hz) at mode no. 5 for configuration of Model in all cases

Frequency (Hz) at mode no. 5 for different configuration							
MODE NO	BASE MODEL	CASE 1	CASE 2	CASE 3	CASE 4		
5	1936.7	5317.8	4312	6297.7	8107.9		

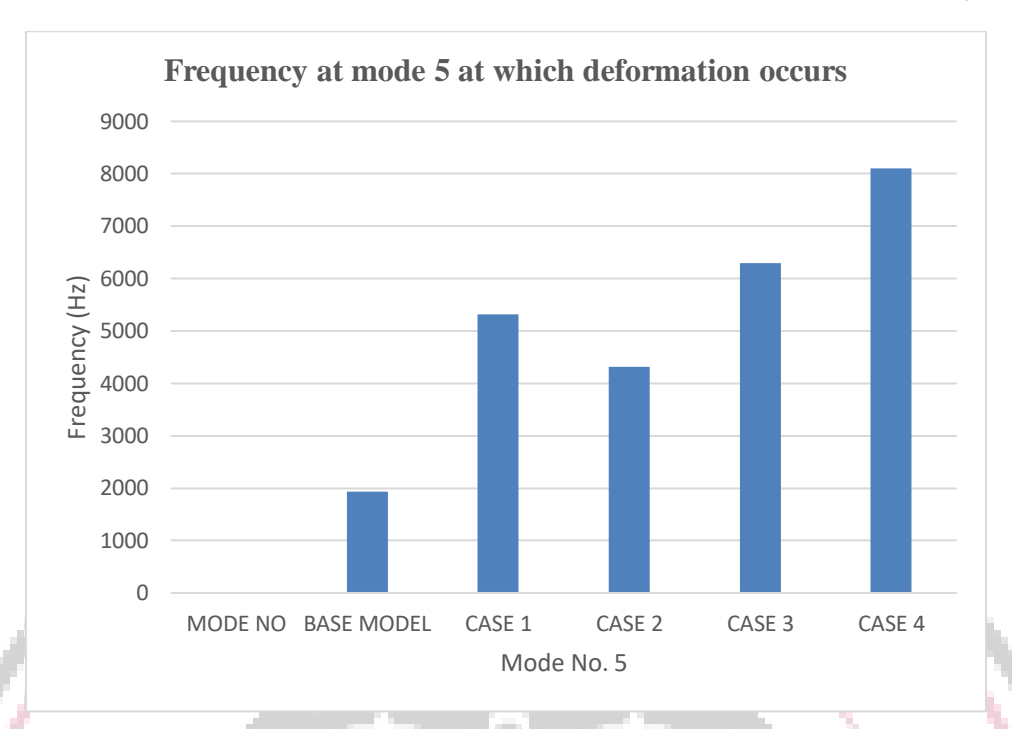


Figure 31 Frequency at mode 5 at which deformation occurs

The above figure shows the in case 4 after attaining maximum frequency of 8107.9 (Hz) deformation takes place which is much better as compared to precious other designs and base model design

#### VI. CONCLUSION

his study investigates how rubber dampers influence NVH and thermal performance in automotive applications through comprehensive simulations and experimental modal analyses. Results indicate that rubber dampers effectively reduce vibration amplitudes and attenuate engine noise, thereby enhancing overall vehicle comfort and performance. Designs incorporating rubber dampers exhibit improved natural vibration frequencies and reduced noise levels compared to baseline configurations with conventional dampers. This underscores the critical role of optimized vibration characteristics in enhancing engine design and highlights the practical benefits of rubber dampers in achieving superior NVH control and thermal efficiency. Future research should focus on further optimizing damping technologies to continually improve automotive NVH management and thermal regulation.

#### REFERENCES

- [1] Abd-el-Malek, M.; Abdelsalam, A.K.; Hassan, O.E. Induction motor broken rotor bar fault location detection through envelope analysis of start-up current using Hilbert transform. Mech. Syst. Signal Process. 2017, 93, 332–350.
- [2] Mehrjou, M.R.; Mariun, N.; Marhaban, M.H.; Misron, N. Rotor fault condition monitoring techniques for squirrel-cage induction machine—A review. Mech. Syst. Signal Process. 2011, 25, 2827–2848.
- [3] Han, T.; Yang, B.-S.; Choi, W.-H.; Kim, J.-S. Fault diagnosis system of induction motors based on neural network and genetic algorithm using stator current signals. Int. J. Rotat. Mach. 2006, 2006, 61690.
- [4] Toma, R. N., Prosvirin, A. E., & Kim, J. M. (2020). Bearing fault diagnosis of induction motors using a genetic algorithm and machine learning classifiers. Sensors, 20(7), 1884.
- [5] R. Marino, S. Peresada and P. Valigi, "Adaptive input-output linearizing control of induction motors," in IEEE Transactions on Automatic Control, vol. 38, no. 2, pp. 208-221, Feb. 1993, doi: 10.1109/9.250510.
- [6] X. Liang, M. Z. Ali and H. Zhang, "Induction Motors Fault Diagnosis Using Finite Element Method: A Review," in IEEE Transactions on Industry Applications, vol. 56, no. 2, pp. 1205-1217, March-April 2020, doi: 10.1109/TIA.2019.2958908.
- [7] Yakhni, M. F., Cauet, S., Sakout, A., Assoum, H., Etien, E., Rambault, L., & El-Gohary, M. (2023). Variable speed induction motors' fault detection based on transient motor current signatures analysis: A review. Mechanical Systems and Signal Processing, 184, 109737.https://doi.org/10.1016/j.ymssp.2022.109737
- [8] Aziz, A.G.M.A.; Abdelaziz, A.Y.; Ali, Z.M.; Diab, A.A.Z. A Comprehensive Examination of Vector-Controlled Induction Motor Drive Techniques. Energies 2023, 16, 2854. <a href="https://doi.org/10.3390/en16062854">https://doi.org/10.3390/en16062854</a>

- [9] Karupusamy, S., Mustafa, M.A., Jos, B.M. et al. Torque control-based induction motor speed control using Anticipating Power Impulse Technique. Int J Adv Manuf Technol (2023). <a href="https://doi.org/10.1007/s00170-023-10893-5">https://doi.org/10.1007/s00170-023-10893-5</a>
- [10] S. P. Biswas, M. S. Anower, S. Haq, M. R. Islam, M. A. Rahman and K. M. Muttaqi, "A New Level Shifted Carrier Based PWM Technique for a Cascaded Multilevel Inverter Based Induction Motor Drive," in IEEE Transactions on Industry Applications, vol. 59, no. 5, pp. 5659-5671, Sept.-Oct. 2023, doi: 10.1109/TIA.2023.3279359.
- [11] Karupusamy, S., Mustafa, M.A., Jos, B.M. et al. Torque control-based induction motor speed control using Anticipating Power Impulse Technique. Int J Adv Manuf Technol (2023). <a href="https://doi.org/10.1007/s00170-023-10893-5">https://doi.org/10.1007/s00170-023-10893-5</a>
- [12] Tran, M. Q., Amer, M., Abdelaziz, A. Y., Dai, H. J., Liu, M. K., & Elsisi, M. (2023). Robust fault recognition and correction scheme for induction motors using an effective IoT with deep learning approach. Measurement, 207, 112398. https://doi.org/10.1016/j.measurement.2022.112398
- [13] Attar, H., Abu-Jassar, A.T., Lyashenko, V. et al. Proposed synchronous electric motor simulation with built-in permanent magnets for robotic systems. SN Appl. Sci. 5, 160 (2023). https://doi.org/10.1007/s42452-023-05375-y
- [14] Saxena, A., Kumar, R., Rawat, A. K., Majid, M., Singh, J., Devakirubakaran, S., & Singh, G. K. (2023). Abnormal Health Monitoring and Assessment of a Three-Phase Induction Motor Using a Supervised CNN-RNN-Based Machine Learning Algorithm. Mathematical Problems in Engineering, 2023(1), 1264345.

